

See discussions, stats, and author profiles for this publication at: <https://www.researchgate.net/publication/280301611>

Online processing of shape information for control of grasping

Article *in* Experimental Brain Research · July 2015

Impact Factor: 2.04 · DOI: 10.1007/s00221-015-4380-z

CITATIONS

3

READS

45

2 authors:



Zhongting Chen

The University of Hong Kong

10 PUBLICATIONS 4 CITATIONS

SEE PROFILE



Jeffrey A Saunders

The University of Hong Kong

46 PUBLICATIONS 1,056 CITATIONS

SEE PROFILE

Online processing of shape information for control of grasping

Zhongting Chen¹ · Jeffrey A. Saunders¹ 

Received: 13 April 2015 / Accepted: 4 July 2015
© Springer-Verlag Berlin Heidelberg 2015

Abstract When picking up objects, we tend to grasp at contact points that minimize slippage and torsion, which depend on the particular shape. Normally, grasp points could be planned before initiating movement. We tested whether grasp points can be determined during online control. Subjects reached to grasp virtual planar objects with varied shapes. On some trials, the object was changed during movement, either rotated by 45° or replaced with a different object. In all conditions, grasp axes were well adapted to the target shape, passing near the center of mass with low force closure angles. On perturbed trials, corrective adjustments were detectable within 320 ms and were toward the same grasp axes observed on unperturbed trials. Perturbations had little effect on either kinematics or the optimality of final grasp points. Our results demonstrate that the visuomotor system is capable of online processing of shape information to determine appropriate contact points for grasping.

Keywords Visuomotor · Reaching · Grasping · Shape

Introduction

To grasp an object in a stable manner that allows manipulation, the visuomotor system must take into account the shape of the object. One common method of grasping small objects for fine manipulation is a two-finger ‘precision grip’ (Landsmeer 1962; Napier 1956). For any given object,

there is generally a limited set of contact points that would allow a stable two-finger grip, and these contact points depend on the specific shape of an object (Blake and Brady 1992; Ponce et al. 1993; Sanz et al. 1998). Previous studies have found that human grasping with a precision grip is sensitive to the constraints posed by object shape (Goodale et al. 1994a, b; Kleinhoddermann et al. 2013; Lederman and Wing 2003). This ability to grasp objects at appropriate contact points would require visual processing of shape information.

In this study, we investigate whether the visuomotor system is capable of online processing of shape information to adaptively adjust grasp points during an ongoing movement. In normal circumstances, the goal positions of the fingers for grasping an object could be determined in a planning phase prior to movement. As long as the object is rigid and stationary, there would be no need to re-compute the goals of the fingers during the movement phase. On the other hand, if the visuomotor system has fast shape-processing mechanisms for control of grasping, it may be possible to generate new target grasp points during online control.

We tested online processing of shape information for control of grasping using a perturbation paradigm, as illustrated in Fig. 1. Subjects made grasping movements toward a virtual object that could be changed during ongoing movements. On perturbed trials, the virtual object was unexpectedly rotated by $\pm 45^\circ$ (Experiment 1) or changed to an entirely different object (Experiment 2), and subjects had to adjust their movement to adapt to the new orientation or shape. The object rotations in Experiment 1 were large enough that subjects would be expected to grasp the objects at different contact points. The perturbations occurred when the index finger was 20 cm away from the target, at which point the hand was moving at near-peak

✉ Jeffrey A. Saunders
jsaun@hku.hk

¹ Department of Psychology, University of Hong Kong, Hong Kong, Hong Kong SAR

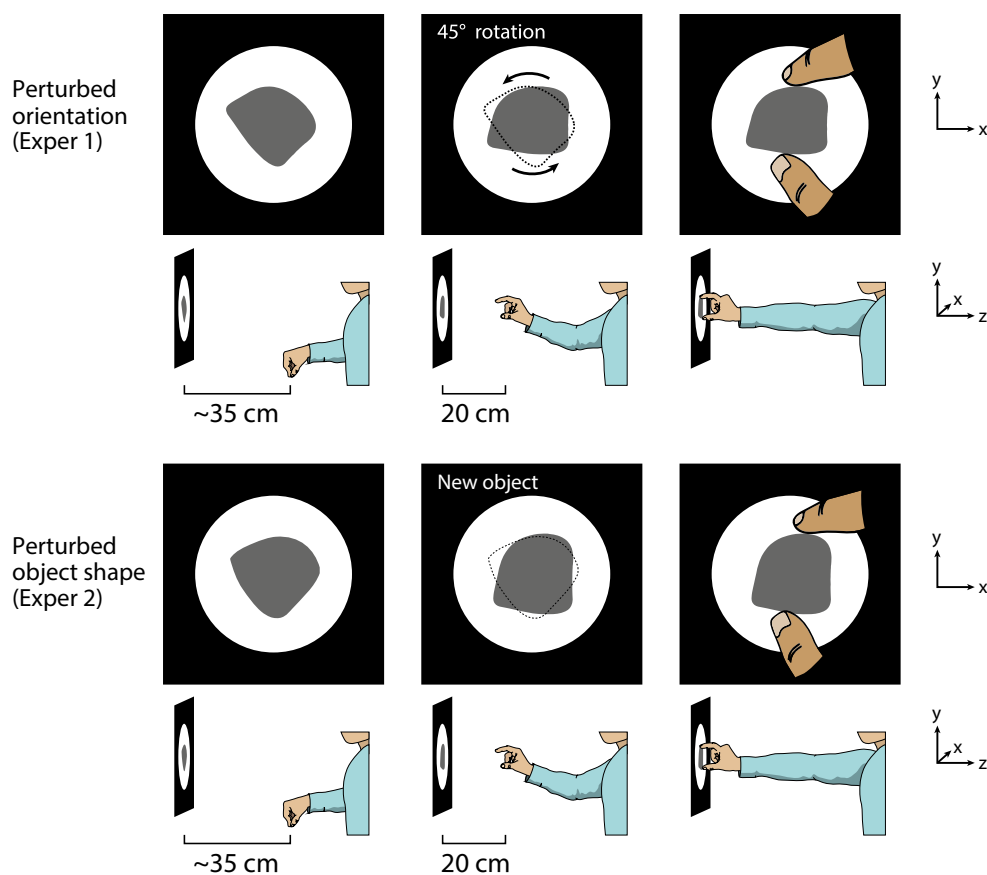


Fig. 1 Illustration of the perturbation conditions in Experiments 1 and 2. Subjects reached to touch virtual 2D objects as they would if grasping. The objects were back-projected onto a projection surface, and sensors attached to the right index finger and thumb tracked movement. In perturbed conditions of Experiment 1 (*top*), the object

was rotated by $\pm 45^\circ$ when the index finger was 20 cm away from the target. In the perturbed conditions of Experiment 2 (*bottom*), the initial object was replaced by a different random object. On perturbed trials, subjects were asked to adjust their movement to touch the screen where they would grasp the new target object

velocity. To achieve appropriate grasp points on perturbed trials without restarting the movement and increasing duration, subjects would have to make online corrections.

Constraints on grasp points

There are two main physical constraints on stable grasping with two-finger precision grip, as illustrated in Fig. 2. One constraint is force closure: The direction of force from the fingers should be close to the orientation of the surface normal at the contact points in order to avoid slippage. To manipulate an object with a precision grip, it is also beneficial for the grasp axis to pass through the center of mass of an object in order to avoid unnecessary torque. For complex objects, there would generally be a limited set of grasp axes that would satisfy both of these constraints.

Some previous evidence indicates that humans are able to grasp complex objects in optimal manner. Bingham and Muchisky (1993a, b) found that subjects were able to identify the center of mass in various planar objects accurately,

as would be required to minimize torque when lifting an object. Some studies of grasping objects with a precision grip have found that subjects do tend to use grasp axes that pass near the center of mass (Goodale et al. 1994a, b; Lederman and Wing 2003). Goodale et al. (1994a, b) also observed that subjects tended to grasp irregular smooth objects at regions with maximum or minimum concavity, which would be likely to have good force closure. These results indicate that subjects are capable of selecting grasp points that are appropriate for the particular shape of an object.

A recent study by Kleinholdermann et al. (2013) measured grasp points for objects with various shapes and orientations and used the results to fit a model of human grasp point selection. The model includes the physical constraints along with a tendency toward a preferred natural grip axis that is independent of object shape and a tendency to minimize movement distance. Simple objects were used to estimate the relative weighting of these factors, and the model was validated using performance for more complex objects. Their results

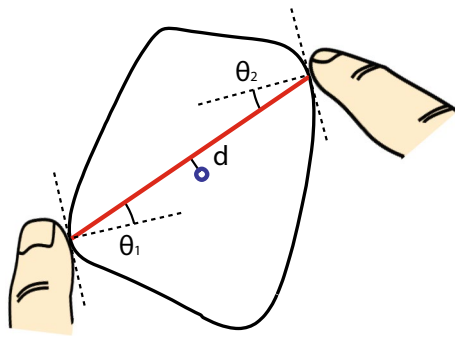


Fig. 2 Illustration of two physical constraints for a stable two-finger grip, force closure and torque control. Force closure requires that the direction of force between the fingers (*red line*) be close to perpendicular to the surface of the object. The angles between the grasp axis and the surface normal directions at the contact points (θ_1 and θ_2) provide a measure of deviation from force closure. If these angles are too large, the object may rotate or slip when force is applied. The tolerable range of θ_1 and θ_2 depends on the friction coefficient of the object's surface. To minimize torque when an object is moved, it is also desirable for the grasp axis to pass through the object's center of mass. The distance (d) from grasp axis to the center of mass (*blue circle*) provides a measure of deviation from optimal torque control. If this distance is too large, then pressure would have to be applied to avoid rotation of the object around the grasp axis when the object is moved (color figure online)

suggest that all these factors contribute to determining the grasp points of complex objects, with force closure and natural grip axis having more influence than the constraint that the grasp axis passes through the center of mass.

For our experiment, we generated target objects with random 2D shapes that varied in their ideal grasp points. Figure 3 shows examples of the shapes along with predicted optimal grasp points based on the Kleinholdermann et al. (2013) model. The optimal axes are highly dependent on the specific shape of the objects. Visual analysis of object shape would therefore be required to grasp these shapes at appropriate contact points.

We measured the optimality of subjects' grasp points with respect to force closure and torque control and compared performance for unperturbed and perturbed conditions. Based on previous results, we expected grasp points on unperturbed trials to be well adapted to the shape of the objects. If the visuomotor system is capable of identifying appropriate grasp points online, then performance on perturbed trials would show similar optimality.

Previous studies of online control of reaching and grasping

Many previous studies have demonstrated online processing of visual information for control of hand movements during reaching and grasping. Online adjustments in response to perturbations have been observed for the

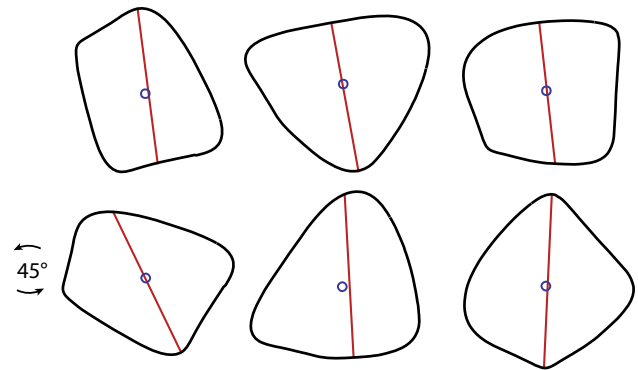


Fig. 3 Examples of target objects used in the experiments and potential grasp axes based on the model of Kleinholdermann et al. (2013). The objects were smooth, random 2D shapes with no deep concavities. Each individual object was presented at two orientations in the image plane that differed by a 45° rotation (*top* and *bottom* rows). The predicted axes (*red lines*) optimize an error measure that combines deviations from force closure, deviation of the grasp axis from the center of mass (*small circles*), and deviation from a natural grip axis for the hand. Here we assume a natural grip axis of 100° from horizontal, which was the average grasp axis observed in our data, and an object weight of 30 g. One can see that the predicted contact points and grasp axis angles depend on the shape of the individual objects as well as their orientation. For some objects, the 45° rotation would be expected to change the grasp axis in a counterclockwise direction (*left*), while for other objects, the grasp axis would be expected to change in a clockwise direction (*middle* and *right*). If an initial target object were replaced by a different randomly chosen object, as in Experiment 2, the change in predicted grasp axis would vary randomly depending on the particular objects (color figure online)

target position (e.g., Bridgeman et al. 1979; Paulignan et al. 1991a; Gentilucci et al. 1992), hand position (Saunders and Knill 2003, 2004, 2005), target orientation (Desmurget and Prablanc 1997; Tunik et al. 2005; Fan et al. 2006; Voudouris et al. 2013), and target size (Paulignan et al. 1991b; Glover et al. 2005; Hesse and Franz 2009; van de Kamp et al. 2009; Karok and Newport 2010).

Perturbations of object shape during reach-to-grasp movements have also been tested. Eloka and Franz (2011) tested conditions in which a disk-shaped target changed to a bar during a grasping movement or vice versa. With no perturbations, subjects showed larger maximum grip aperture when reaching to grasp a bar than when reaching to grasp a disk with matched width. When the shape was perturbed early in the movement, the maximum grip aperture changed to be consistent with the new target object. Another study by Ansuini et al. (2007) tested perturbed conditions in which an object with concave 2D shape was replaced by an object with convex 2D shape during a grasping movement or vice versa. They observed modulation of hand shape in response to perturbations, which could be due to online control. In their study, however, movement durations were relatively long and increased with perturbations (1326 vs.

1450 ms), so the corrections might reflect re-initialization of the movement rather than online control.

While these studies demonstrate responses to shape perturbations, the responses did not necessarily require detailed analysis of object shape. Both Ansuini et al. (2007) and Eloka and Franz (2011) used a limited set of symmetric objects, and the perturbations required changes in grip aperture rather than change in the orientation of the grasp axis. Thus, the perturbation responses might not reflect the use of shape information to determine appropriate contact points that satisfy physical and postural constraints.

A recent study by Voudouris et al. (2013) demonstrated online adjustment to grasp points in response to perturbations of object orientation. Subjects reached to grasp either a cube or ball, which on perturbed trials was rotated by 12° during the movement. For the cube, subjects generally rotated their hand in the same direction of the object rotation to maintain the same grasp points, but sometimes rotated in the opposite direction toward a different set of grasp points. These responses demonstrate that the visuomotor system is capable of determining new target grasp points even after movement has initiated. However, this did not necessarily require online processing of object shape, because the same two objects with simple symmetric shapes were used throughout the experiment and were visible prior to the perturbations of object orientation.

Online shape processing for grasping

Our conditions and analysis tested whether the visuomotor system can identify appropriate grasp points for a complex shape during an ongoing movement. The rotation perturbations in Experiment 1 were similar to the conditions of Voudouris et al. (2013) in that the shape of the target object was not perturbed. However, the expected change in grasp axis in our conditions varied depending on object shape (see Fig. 3), while in the previous study it was constant. The conditions in our Experiment 2 were even less predictable. The new target shape was randomly chosen and only visible after movement was initiated, so grasp points would have to be determined entirely during the online control phase. In both experiments, appropriate grasp points for the final target object on perturbed trials could not be determined in advance and would depend on the particular shape of the object.

We took advantage of the differences in grasp points across different shapes to determine whether adjustments to grasping on perturbed trials were toward the same grasp points used on unperturbed trials. If the visuomotor system is capable of online processing of object shape to determine appropriate grasp points, then the grasp points on perturbed trials would be similar to the grasp points on unperturbed objects with the same final target object. However, other

strategies are possible. For example, subject might respond to perturbations by grasping at points on the boundary of the new object that are close to the target grasp point on the original object. We used results from unperturbed trials to determine the expected grasp points for the initial and final target objects on perturbed trials and performed a regression analysis to determine to the extent that the observed grasp points were predicted by either the initial or final object. If the final object is a significant predictor of grasp points on perturbed trials, this would indicate that perturbation responses were toward the same preferred grasp points as on unperturbed trials.

We used the same approach to analyze dynamic adjustments to the orientation of the hand in response to perturbations. When reaching to grasp an object, subjects gradually adjust the orientation of the hand over the course of movement in preparation for the final grasp points (Mamassian 1997; Greenwald and Knill 2009). If the hand were controlled in a similar way on perturbed trials, then the initial responses to perturbations would be toward the grasp points used on unperturbed trials with the same final target object. The grasp points observed on unperturbed trials would therefore be a predictor of dynamic adjustments on perturbed trials. If initial perturbation responses were not shape specific, then this relation would not be present. We also compared the speed and duration of hand movements in perturbed and unperturbed conditions to test whether perturbation responses caused delays or other changes to the movement kinematics.

Methods

Participants

Ten right-handed subjects with normal or corrected-to-normal vision were recruited from the University of Hong Kong for each experiment and were paid for their participation. The procedures were approved by the Human Research Ethics Committee for Non-Clinical Faculties.

Apparatus and stimuli

The stimuli were computer-generated images of 2D shapes back-projected on an acrylic surface by BenQ 710ST DLP projector with a resolution of 1920 × 1080 pixels and a refresh rate of 60 Hz. Images were rendered with OpenGL using a NVIDIA Quadro 600 graphics card and were antialiased with sub-pixel resolution. The projection surface was rigid and semitransparent and was aligned to be perpendicular to the floor and the subject's line of sight, at a distance of 50 cm from the subject's eyes. A black board with circular aperture was placed on top of the projection

surface to create a 16.8-cm-diameter visible region that was centered in front of the subjects. Subjects were seated at a table and allowed free movement of their head. The starting position for the hand was a marked location on the table, and the hand was visible throughout movements.

The movement of the index finger and thumb of a subject's right hand was recorded at 240 Hz with 3D Guidance trakSTAR system. A sensor was attached to back of the fingernails using latex finger cots, which wrapped over the tip of the finger and the sensor. A calibration procedure was used to estimate the position of the contact surface of each finger relative to the position of the corresponding sensor.

The stimuli were smooth, random 2D shapes presented in gray on a black ground. To create a shape, we first generated a random polygon by computing the convex hull of 5–7 random vertices and then applied Gaussian blur to the radial function ($\sigma = 17^\circ$). A total of 16 unique shapes were generated in this way. Across shapes, the average radius was 2.40 cm (± 0.229 cm) and the average area was 18.55 (± 3.54) cm².

Procedure

The task of a subject on each trial was to reach and touch a virtual object in the way that they would if they were grasping the object. At the start of a trial, the subject's hand was at a starting location that was approximately 40 cm away from the surface. The presentation of a stimulus was the cue for them to begin movement. Subjects reached to touch the object, making contact with the projection surface, and then held their hand at the end position until the stimulus disappeared. There was no speed requirement, but subjects were encouraged to move immediately after stimulus presentation and avoid explicitly thinking about their movement. They were instructed to try to do the task as if they were grasping an object in daily life. Despite the unnatural demands of the perturbed conditions, subjects found the task easy to perform, and the time course of movements was similar to that observed in a pilot study with no perturbed conditions.

On perturbed trials in Experiment 1, the object was rotated within the image plane by $\pm 45^\circ$ at the moment when the index finger became less than 20 cm away from the projection surface, as measured in the depth direction. The perturbed trials in Experiment 2 were the same except that the shape of the object was changed to that of a different, randomly chosen object when the index finger reached 20 cm away from the projection surface. For perturbed trials, subjects were instructed to adjust their movement to grasp the object in the new position. To familiarize themselves with the task, subjects performed 12 practice trials that included both unperturbed and perturbed conditions.

For each object, we arbitrarily defined a base orientation within the image plane. On unperturbed trials, the object could either appear at this base orientation (0°) or at an orientation that differed by a 45° rotation. On perturbed trials in Experiment 1, the object would either start at the base orientation and the change to the 45° orientation, or vice versa. On perturbed trials in Experiment 2, the initial object was replaced by a different object at either the 0° or 45° orientation, chosen randomly.

In both experiments, subjects performed a total of 320 trials in a 1-h session, with breaks provided every 32 trials. Each of the 16 individual objects was presented 10 times without perturbations and 10 times with perturbations. In Experiment 1, there were an equal number of unperturbed trials with each base orientation (0° and 45°) and an equal number of perturbed trials with positive rotation (0° – 45°) and negative rotation (45° – 0°). In Experiment 2, each object appeared as the final target on an equal number of trials, with half at each base orientation. The order of conditions was randomized across the whole session.

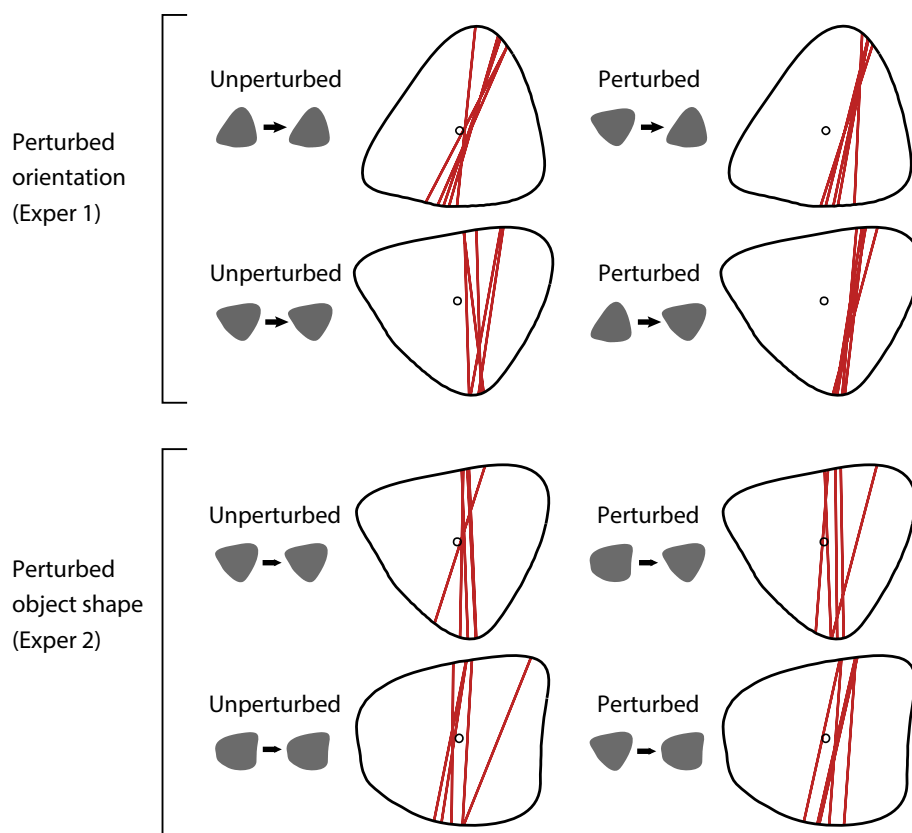
Before the experimental trials, subjects performed a calibration procedure in which they touched the projection surface at seven sets of target locations indicated by small dots. The 3D sensory positions were compared to the targets to estimate the displacement from the sensors to the fingertips. For validation, the sequence of target locations was presented twice. The calibration procedure was repeated until the RMS error between the first and second set of sensor positions was less than 4.5 mm.

Results

Grasp axes for unperturbed and perturbed trials

Figure 4 shows examples of grasp axes from individual trials of a representative subject from Experiment 1 (top) and from Experiment 2 (bottom). The final grasp axis on a trial was computed from the finger positions immediately after the fingers stopped moving in depth due to contact with the projection surface. The left figures show grasp axes from individual trials in the unperturbed conditions, and the right figures show grasp axes on perturbed trials with the same post-perturbation target object. From the unperturbed trials in Experiment 1, one can see that the grasp axes depended on the orientation of the object, differing in relation to the object as well as relative to the image plane. The grasp axes on perturbed trials were similar to unperturbed trials with the same object and orientation at the end of the trials (left vs. right). The final grasp points in Experiment 2 also show a consistency across unperturbed and perturbed conditions. Although the target object was not visible at the start of movement on perturbed trials in Experiment 2 and

Fig. 4 Final grasp axes for samples objects from one subject in Experiment 1 (*top*) and Experiment 2 (*bottom*). The *left figures* show the grasp axes in unperturbed conditions, and the *right figures* show grasp axes for perturbed conditions with the same final object and orientation



was not predictable, the final grasp axes appear similar to those used in unperturbed trials with the same target object. This consistency suggests that movement corrections in response to perturbations were toward appropriate grasp points for the post-perturbation target object.

To quantitatively evaluate whether grasp axes for perturbed trials were adjusted to be consistent with the post-perturbation object, we performed a regression analysis using the expected grasp axes for the initial stimuli and post-perturbation stimuli as predictors. We fit a linear model to the perturbed trials from each subject:

$$\alpha_{\text{pert}} = \beta_0 + \beta_1\alpha_1 + \beta_2\alpha_2 + \text{noise} \quad (1)$$

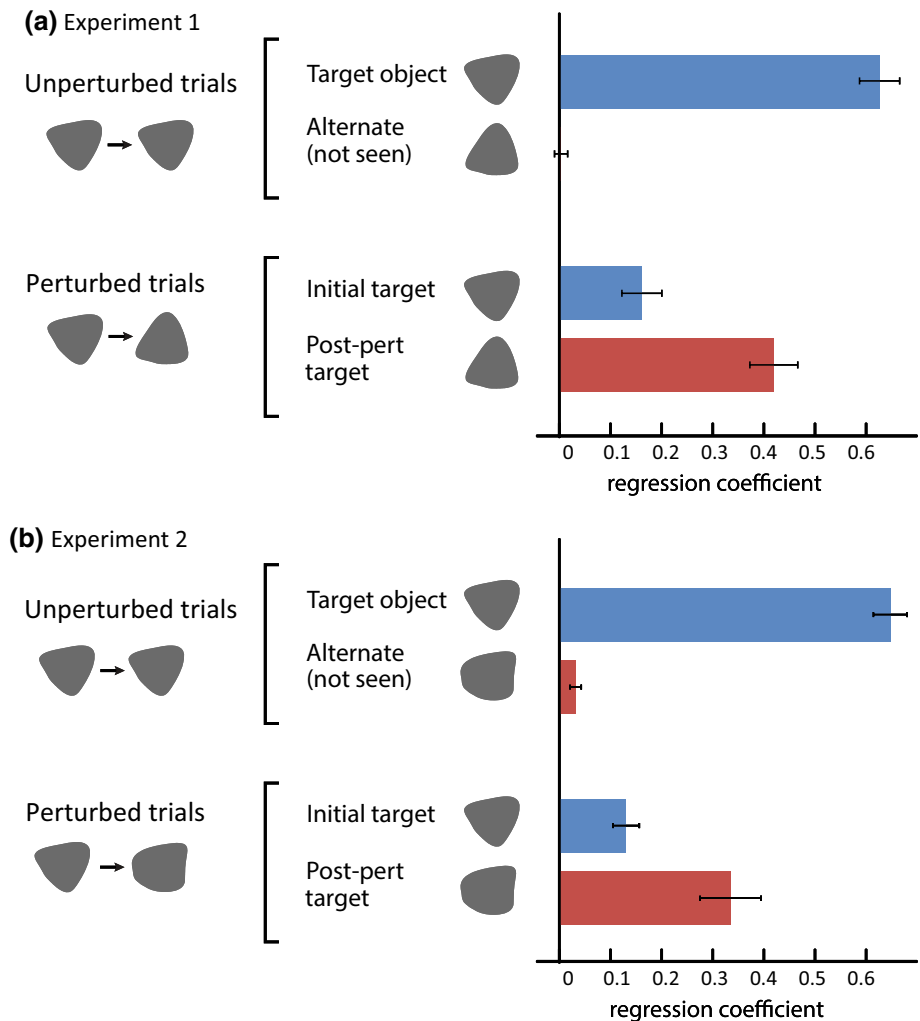
where α_{pert} is the angle of the final grasp axis on a given perturbed trial, α_1 and α_2 are the grasp axis angles that would be expected for the initial orientation and post-perturbation orientation of the object for an individual trial, and β_1 and β_2 are regression coefficients representing the relative influence of the stimuli presented before and after the perturbation. The expected grasp axis angles (α_1 and α_2) were computed by averaging final grasp angles for each subject and object from the unperturbed trials. For comparison, we also applied the regression analysis to data from unperturbed conditions, setting α_1 to be the expected grasp axis for the presented stimulus and α_2 to be the expected grasp axis for the other orientation of the

object that was not presented (Experiment 1), or a random alternative object (Experiment 2). The regression results for unperturbed trials provide an indication of the range of coefficients that would be expected if the grasp axes were entirely determined by a single object, given the variability across trials in the same condition.

Figure 5 shows the means of the fitted coefficients, averaged across subjects, for Experiment 1 (a) and Experiment 2 (b). The results from the unperturbed trials confirm that final grasp axes systematically varied across objects. In both experiments, the average grasp axis for the presented stimuli was highly predictive of grasp axes on individual unperturbed trials, while the regression weights for the unseen alternative stimuli were negligible. For the perturbed trials, the initial stimuli and the post-perturbation stimuli were both significant predictors for final grasp axes ($p \leq .003$), but the post-perturbation stimuli was a significantly stronger predictor (Experiment 1: $t(9) = 4.09$, $p = .003$; Experiment 2: $t(9) = 3.11$, $p = .012$). These results provide evidence that perturbation responses were toward the grasp axes that would be expected for the object and orientation that was presented after perturbation, and that subjects only partially corrected their movements.

For Experiment 1, we performed another analysis to test whether subjects tended to switch to a new grasp axis on perturbed trials or rotate their hand to grasp at the object

Fig. 5 Mean regressed coefficients when fitting the final grasp axes as a linear function of the expected grasp axes from initial and post-perturbation stimuli for Experiment 1 (a) and Experiment 2 (b). The *top set of bars* in each graph shows the results of the control analysis of unperturbed trials, in which one predictor was the expected grasp axis from the presented target and the other was the expected grasp axis from the alternate target that was not presented. The *lower set of bars* show the results from the analysis of perturbed trials, in which the predictors were the expected grasp axis from initial stimuli and the post-perturbation stimuli. *Error bar* depicts one standard error of the means. One can see that the grasp axes on the perturbed trials were more correlated with the expected grasp axes of the post-perturbation stimuli than the initial stimuli



at the original target points. If subjects rotated their hand along with the perturbation, the difference between the final grasp axis (α_{pert}) and expected grasp axis for the stimuli before perturbation (α_1) would be $\pm 45^\circ$. The observed change in grasp axis was consistently less than 45° , averaging $18.1^\circ \pm 14.9^\circ$ SD, and there was no indication of bimodality in responses. This indicates that subjects did not simply rotate their hands to follow the rotation of the object on perturbed trials. They instead grasped the object at new contact points for which the grasp axis was near the overall preferred orientation of the hand. The results of the regression analysis suggest that these new target points were the same as on unperturbed trials with the same final stimuli.

Optimality in grasp point selection

We evaluated the optimality of final grasp points for unperturbed and perturbed conditions with respect to both torque control and force closure. As a measure of the optimality of torque control, we used the distance from the grasp axis

to the center of mass (COM) of an object. As a measure of force closure, we computed the angular difference between grasp axis and the normal direction of the contour at each grasp point and then averaged the absolute differences from the index finger and thumb. For each subject, we computed the median COM distance and force closure angle relative to the final stimuli for unperturbed and perturbed conditions. For the force closure measure, we also computed the optimality of grasp axes on perturbed trials relative to the initial object orientation and the optimality of relative to a random object and orientation. These comparison measures indicate the deviations from optimality that would be expected if grasp axes were not adjusted to match the presented stimuli. We did not compute comparison measures for the COM distance because the objects were positioned with their COM at the same central location. Figure 6 shows the mean results, averaged across subjects, for Experiments 1 and 2.

The grasp axes passed close to the COM of the target objects in both unperturbed and perturbed conditions.

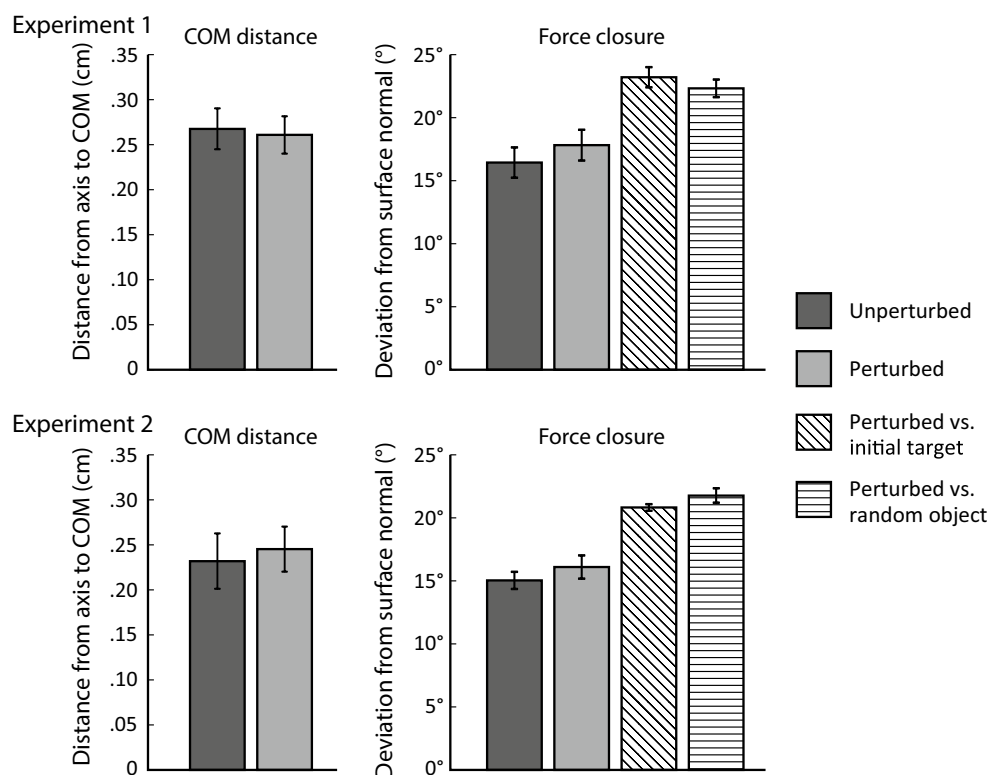


Fig. 6 Optimality of final grasp points in Experiment 1 (*top*) and Experiment 2 (*bottom*) with respect to torque control and force closure. The *left graphs* plot mean distance from the grasp axis to the center of mass, and the *right graphs* plot mean angular deviation between the grasp axis and the surface normal directions. Also shown

are average force closure angles when grasp points from perturbed trials are compared to either the initial target stimuli (*diagonal lines*) or a random different object (*horizontal lines*). Error bars depict standard errors

The average deviation from the COM was only 2.51 mm (± 0.8 mm SD), and there was no significant difference between the unperturbed and perturbed conditions in either Experiment 1 ($t(9) = .49, p = .64$) or Experiment 2 ($t(9) = 1.53, p = .159$). The results indicate that subjects did tend to grasp objects along axes that are optimal for torque control. However, because the objects were presented with their COM at a constant location, the COM distance does not provide a strong test of the optimality in perturbed conditions compared to unperturbed conditions. The precise alignment of the grasp axes on unperturbed trials suggests that the COM constraint did contribute to movement planning, but we cannot determine the extent that the COM of the post-perturbation stimuli contributed to adjustment of grasp points on perturbed trials. While this aspect of our results is ambiguous, it is clear that subjects were able to adjust their movements in response to perturbations without reducing the optimality of grasp axes with respect to torque control.

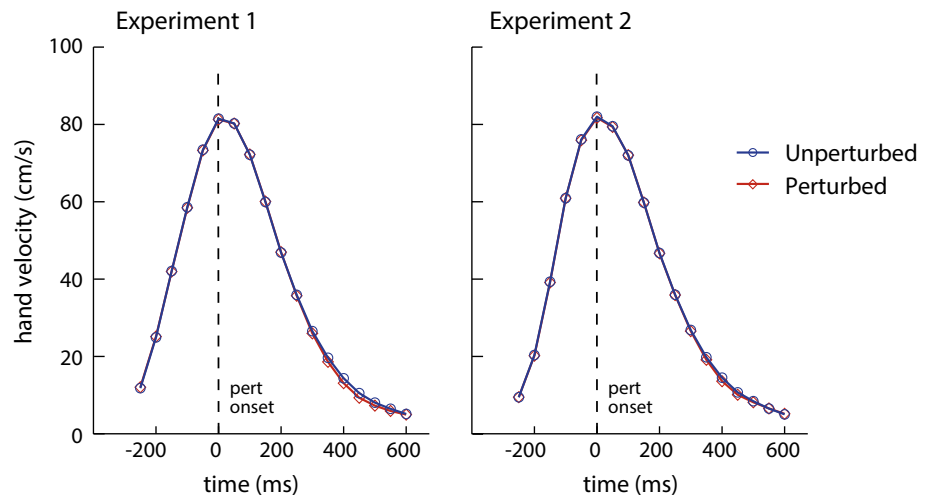
Grasp axes were also close to optimal with respect to force closure. In Experiment 1, the force closure angles averaged $16.43^\circ (\pm 3.82^\circ \text{ SD})$ in unperturbed condition and $17.82^\circ (\pm 3.84^\circ \text{ SD})$ in perturbed condition. This difference

was small but significant ($t(9) = 2.54, p = .033$), indicating less optimal force closure in the perturbed conditions. In Experiment 2, the average force closure angle was similar in magnitude, averaging $15.03^\circ (\pm 2.14^\circ \text{ SD})$ in the unperturbed condition and $16.10^\circ (\pm 2.91^\circ \text{ SD})$ in the perturbed condition, with no significant difference between the unperturbed and perturbed conditions ($t(9) = 1.97, p = .081$).

An ANOVA comparing the optimality in Experiments 1 and 2 found no overall difference in either COM distance ($F(1,18) = .55, p = .47$) or force closure angle ($F(1,18) = 1.24, p = .28$) and no interaction between experiments and perturbation conditions (COM: $F(1,18) = 1.51, p = .23$; force closure: $F(1,18) = .17, p = .68$). In both experiments, perturbations had little or no effect on the optimality of final grasp points.

Figure 6 also shows the force closure angles of grasp axes from perturbed trials when computed relative to the initial pre-perturbation object or a random object. The force closure angles relative to the target object were significantly smaller than relative to the pre-perturbation stimuli (Experiment 1: $t(9) = 3.48, p = .006$; Experiment 2: $t(9) = 5.01, p = .001$) or relative to a random object (Experiment 1: $t(9) = 5.32, p < .001$; Experiment 2: $t(9) = 5.73, p < .001$).

Fig. 7 Hand velocity profiles for unperturbed trials (blue) and perturbed trials (red) in Experiment 1 (left) and Experiment 2 (right). The graphs plot the mean velocity of the hand as a function of time after the perturbation onset point (dashed line). The mean velocity profiles for unperturbed and perturbed trials are almost identical. Error bars depict standard errors (color figure online)



These results indicate that grasp axes were sensitive to the force closure constraint and that the adjustments in response to the perturbations were effective in maintaining the optimality.

Dynamics of perturbation responses

To test whether the perturbations prompted re-initialization of movement or other qualitative changes, we compared the speed profiles and movement durations in the unperturbed and perturbed conditions. Figure 7 shows the mean speed profiles from 250 ms before perturbation to 600 ms after perturbation, averaged across subjects, for perturbed and unperturbed trials in Experiment 1 (left) and Experiment 2 (right). The speed profiles are almost identical in the unperturbed and perturbed conditions. To test this statistically, we compared the average speeds within 50-ms windows of time. In Experiment 1, there were no significant differences in speed at any time window ($p \geq .08$). In Experiment 2, we detected a small difference in movement speed at two time windows, 275–325 ms (19.61 vs. 19.10 cm/s, $t(9) = 2.45$, $p = .037$) and 325–375 ms (14.35 vs. 13.48 cm/s, $t(9) = 3.35$, $p = .009$), and no other significant differences ($p \geq .057$). These limited effects suggest that perturbation responses were smooth and did not require qualitative changes in movement strategy. We also compared the overall movement durations and the durations of the final portion of the movement. The final movement duration was measured from when the finger was 20 cm away from the target, which is the trigger for perturbation, until contact of a finger with the projection screen. The duration of the final movement phase was longer in the perturbed conditions (Experiment 1: $t(9) = 3.29$, $p = .009$; Experiment 2: $t(9) = 3.11$, $p = .013$), but the differences were small: 861 versus 922 ms in Experiment 1 and 878 versus 916 ms in Experiment 2. Similarly, the overall movement durations

showed a small but significant difference (Experiment 1: 1132 vs. 1195 ms, $t(9) = 3.28$, $p = .010$; Experiment 2: 1148 versus 1184 ms, $t(1) = 2.97$, $p = .016$). These results show that the perturbations had only minimal effect on the time course of movements, which suggests that normal online control mechanisms were responsible for the perturbation responses.

We further investigated the kinematics of perturbation responses by analyzing how the axis between the index finger and thumb changed over the course of movement. The linear regression model described previously was modified to analyze grasp axes on perturbed trials at different moments in time:

$$\alpha_{\text{pert}}(t) = \beta_0(t) + \beta_1(t)\alpha_1 + \beta_2(t)\alpha_2 + \text{noise}, \quad (2)$$

where $\alpha_{\text{pert}}(t)$ is the grasp axis angle at a given time t , α_1 and α_2 are the grasp axis angles that would be expected for the initial and post-perturbation stimuli for each individual trial (same as before), and $\beta_1(t)$ and $\beta_2(t)$ are regression coefficients representing the relative influence of the initial and post-perturbation stimuli at time t .

One complication is that the 3D orientation of the hand changes systematically over the course of the movement, irrespective of the final grasp axis. At the start of movement, the axis from the thumb to the finger was oriented in the depth direction, and over time this axis was rotated into the frontal plane. If subjects adjust their finger positions early in the movement in preparation for the final grasp axis, the variations in 3D position would not be in the frontal plane.

To associate grasp axes at different points in the movements, we computed a set of moving reference frames for each subject that represents the average positions of the hand at different distances from the target. We extracted frames from different unperturbed trials based on the mean positions of the thumb and index finger to get a set

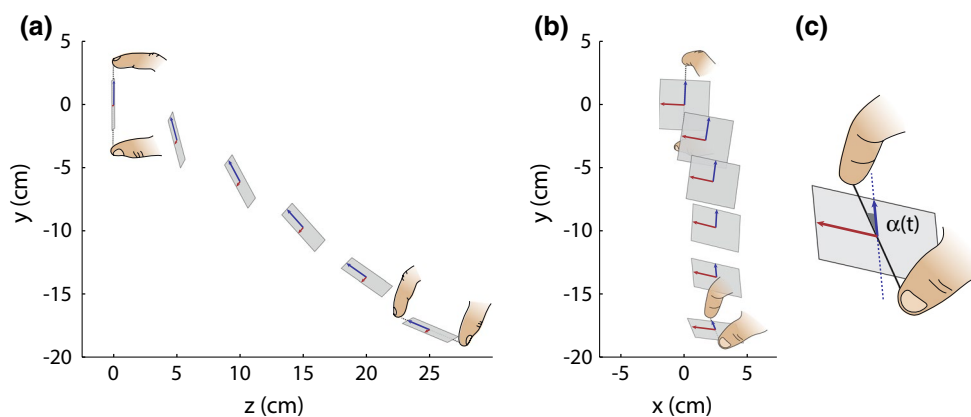


Fig. 8 Example of the moving reference frame representing the average hand position over the course of a trial from a representative subject. The *left graph a* shows a side view and the *middle graph b* shows a view from behind the subject. The *arrows* depict the basis vectors of reference frames at various distances. The *blue* basis vec-

tors correspond to the average 3D orientation of the axis between the thumb and index finger. The *red* basis vectors were the orthogonal direction that showed the largest correlations with the final grasp axes. Grasp axis angles at different points in a movement, $\alpha(t)$, were computed relative to these reference frames **(c)** (color figure online)

of 3D grasp axes at a given distance. The first basis vector of the reference frame was the mean 3D orientation of the grasp axes. The second basis vector was chosen to be the orthogonal direction that was most predictive of the final grasp axis. To compute this direction, we first projected the set of grasp axes onto a plane orthogonal to the mean grasp axis and then computed the best-fitting linear mapping from these residual vectors onto the set of final grasp angles. The gradient direction of the best-fitting map was used as the second basis vector. Trial-to-trial variations of the grasp axis in this direction would be the most strongly predictive of variations in the final grasp axis. The reference frame defined by these basis vectors therefore provides an optimal way to compare orientation of the hand at an early stage in movement to the orientation at the end of movement. This method requires detectable correlations between earlier and final hand orientation. For all subjects, there were significant correlations up to a distance of 25 cm from the target, which allowed computation of stable reference frames over the range of interest. Figure 8 shows an example of the moving reference frame for a representative subject. The reference frames from a subject were used to compute a grasp axis angle at each moment in time over the course of a perturbed trial, $\alpha_{\text{pert}}(t)$, which can be compared to the expected final grasp axis angles from the initial and post-perturbation stimuli, α_1 and α_2 .

Figure 9a plots the mean regression coefficients $\beta_1(t)$ and $\beta_2(t)$ fit to the perturbed trials from Experiment 1 (left) and Experiment 2 (right) using Eq. (2). For this analysis, trials were parameterized as a function of time after perturbation in order to observe the emergence of the perturbation effect as a function of time. The $\beta_1(t)$ coefficient (red) indicates

the correlation between the orientation of grasp axis at time t and the orientation of the final grasp axis expected from the initial pre-perturbation stimuli. At the time of the perturbation onset, the average $\beta_1(t)$ is significantly above zero, indicating that subjects had already begun adjusting the orientation of their hand toward an appropriate grasp axis for the initial stimuli. The average $\beta_1(t)$ coefficient continues to increase until about 310–320 ms after perturbation onset and then begins to decrease. At around the same time, one can see that the $\beta_2(t)$ coefficient (blue) begins to increase from zero. The $\beta_2(t)$ coefficient represents the correlation between the orientation of the grasp axis at time t and the orientation of the final grasp axis expected from the post-perturbation stimuli. An increase in $\beta_2(t)$, coinciding with decrease in $\beta_1(t)$, indicates that the orientation of the hand was being adjusted away from the grasp axis for the pre-perturbation stimuli and toward the grasp axis for the post-perturbation stimuli. The latency of the transition point therefore provides an upper bound on the time required to identify new target grasp points and plan corrective adjustments to movement.

The responses to perturbations of object orientation and object shape were highly similar. The peak of the $\beta_1(t)$ function occurred after an average of 312 ± 42 ms in Experiment 1 and 317 ± 36 ms in Experiment 2. We compared across experiments and found no significant difference in either the latency of the $\beta_1(t)$ peak ($t(18) = .308$, $p = .762$) or magnitude of the peak ($t(18) = .024$, $p = .981$). In both experiments, corrective adjustments toward appropriate grasp points for the perturbed target were detectable within 310–320 ms of perturbation onset.

Figure 9b plots the mean regression coefficients analyzed as a function of normalized time, which shows the

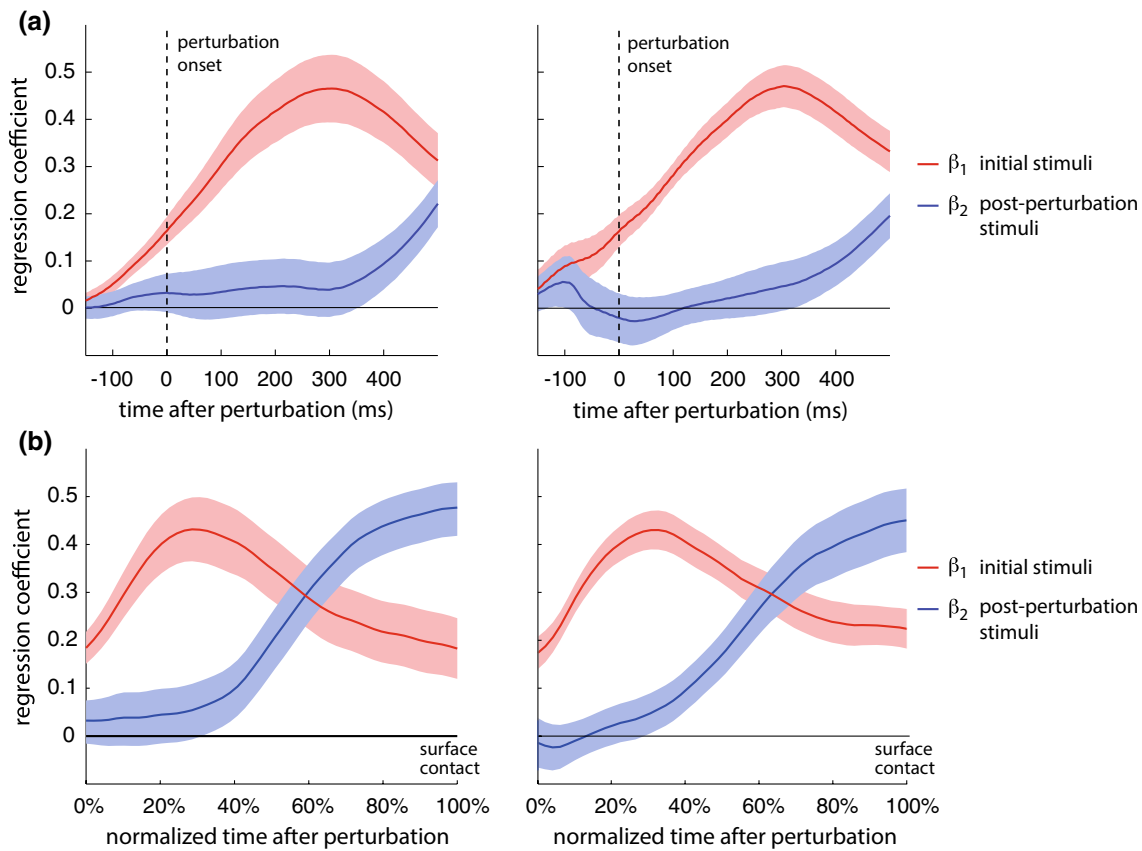


Fig. 9 Influence of the initial stimuli (*red*) and the post-perturbation stimuli (*blue*) on the orientation of the grasp axis over the course of movement in Experiment 1 (*left*) and Experiment 2 (*right*). **a** The *top graphs* plot mean regression coefficients β_1 and β_2 as a function of time before and after perturbation (see text for details). Shaded regions depict ± 1 standard error. The increase in β_1 indicates gradual orienting of the hand toward the expected final grasp axis for the initial stimuli. The average β_1 coefficient begins to decrease around the same time that β_2 begins to increase from zero, indicating adjustment

influence of initial and post-perturbation stimuli over the full range of time from the perturbation onset until the contact with the surface. While adjustments to grasp axis were detectable after a short latency, a substantial portion of the overall adjustment occurred during the final approach of the hand. This is not surprising given the limited distance and time available to adjust movement. When the perturbations occurred, the hand was 20 cm away from the target and moving at a speed of about 80 cm/s, so responses were necessarily during the deceleration portion of the movement. One can see that there was a smooth transition from adjusting toward the predicted grasp axes for the initial stimuli (*red*) to adjusting toward the predicted grasp axes for the post-perturbation stimuli (*blue*), and by the end of movement, the grasp axes were primarily determined by the post-perturbation stimuli.

toward the expected final grasp axis for the post-perturbation stimuli. This transition reflects the corrective responses to the perturbations. **b** The *bottom graphs* plot the regression coefficients as a function of normalized time, ranging from the perturbation onset (0 %) to the moment of contact with the surface (100 %). As the hand approaches the surface, the grasp axis becomes more aligned with the predicted grasp axis for the post-perturbation stimuli than the initial stimuli (color figure online)

Discussion

Optimality of grasp points

The contact points observed in our virtual grasping task were well adapted to the shapes of the various objects and their presented orientation. Grasp axes passed very close to the center of mass of the objects, which is consistent with some previous results for grasping real objects (Goodale et al. 1994a, b; Lederman and Wing 2003). The angular deviation between the force direction and the surface normal was also low, averaging 18°. For most common materials, a force closure angle of less than 30° would be sufficient to avoid slippage (Seo and Armstrong 2009), so the observed grasp axes were well within the range required for a stable grip. The force closure angles were lower than

would be expected if grasp axes were randomly chosen (see Fig. 6), suggesting that this constraint contributed to selection of grasp points for various individual shapes. Our results provide further evidence that visuomotor system is sensitive to the constraints posed by object shape for achieving a stable grip.

The observed grasp axes were generally consistent with a recent analytical model of Kleinhoddermann et al. (2013), who used human grasp points for objects with various shapes to estimate the relative influence of different constraints on grasp point selection. Their results suggested that force closure and preference for a natural grip axis were the dominant influences, with torque control playing a smaller role. We found that force closure angles were lower than would be expected if grasp axes were random, which is consistent with sensitivity to the force closure constraint. We also observed evidence for a preference toward a natural grip axis. In Experiment 1, subjects switched to new grasp points when objects rotated by 45° rather than following the rotation of the object, and in both experiments, the grasp axes for individual subjects tended to have a limited range of orientations ($SD = 17^{\circ}$ – 22°). These aspects of our findings are consistent with the model of Kleinhoddermann et al. (2013). A possible inconsistency is that grasp axes passed very close to the center of mass, which might not be expected if torque control were a weak constraint. However, our objects were not designed to clearly distinguish between different constraints, so this optimality may not have been at the expense of force closure or deviation from the natural grip axis. Our results suggest that all these constraints contribute to grasp point selection, which is in general agreement with the findings of Kleinhoddermann et al. (2013).

Online determination of grasp points

The main goal was to test whether subjects could make online corrections to grasp points during movement. In normal conditions, optimal grasp points could be determined by visual shape processing prior to movement. This was prevented in our perturbed conditions, which changed the orientation or shape of objects in an unpredictable manner when the hand was near-peak velocity.

Our results demonstrate that grasp points can be determined online during movement with little or no cost to performance. On perturbed trials, we found that subjects adjusted their movement to grasp objects at similar contact points as on unperturbed trials with the same object and orientation. The corrections in response to perturbations were smooth and produced only a minimal increase in movement duration (38–61 ms). The grasp points on perturbed trials remained close to optimal with respect to both torque control and force closure. The force closure angles

on perturbed trials in Experiment 1 were slightly larger than for unperturbed trials, but were more optimal than would be expected if subjects had not adjusted their movement in response to perturbations (Fig. 6). Subjects were able to guide their fingers to appropriate grasp points for an object even when the grasp points could not be identified prior to movement.

Our regression analysis of perturbation responses measured adjustments of the hand that were toward the expected grasp axes for the perturbed target object. The observed responses therefore cannot be attributed to general reactions to an unexpected change in the stimuli. The perturbations might have caused some general changes in kinematics due to their unnatural nature. However, any such effects would not be correlated with the expected changes in grasp axes on perturbed trials. The difference between the expected grasp axis for initial and post-perturbation stimuli on perturbed trials depended on the particular shape and orientation of objects, which varied randomly across trials. We used this trial-to-trial variation to detect the component of perturbation responses that were toward appropriate grasp axes for the perturbed target objects. Because the measured responses were toward stimulus-specific grasp axes, rather than general reactions, we can infer that the visuomotor system was able to identify new and appropriate contact points during online control of a movement.

The perturbation responses in Experiment 2 would further require online analysis of object shape. This would not have been necessary in Experiment 1 because the same target object was presented before and after perturbations. In this situation, the visuomotor system could have identified a set of optimal grasp axes for a given shape prior to movement and then switched between predetermined grasp axes in response to the perturbations. In Experiment 2, however, the grasp points on perturbed trials could not have been pre-planned because the target was not visible until the onset of perturbation and could not be anticipated. In these conditions, grasp points that are appropriate for the shape of the new target object had to have been determined during movement.

Some other recent studies have observed online corrections of grasping movements in response to perturbations of object orientation (Fan et al. 2006; Voudouris et al. 2013) and object shape (Ansuini et al. 2007; Eloka and Franz 2011). These studies used objects with simple, symmetric shapes. Our results indicate that subjects can also make online corrections when grasping objects with more complex shapes, for which the optimal contact points are highly dependent on the particular shape.

The dynamics of perturbation responses were highly consistent across experiments. For both perturbations of object orientation and object shape, corrective adjustments were detectable within about 310–320 ms of perturbation

onset. At this time, the influences of the pre-perturbation stimuli began to decrease and the influence of the post-perturbation stimuli began to increase (Fig. 9). In Experiment 1, the same shape was presented before and after perturbations, so preprocessing of object shape could potentially have facilitated computation of new grasp points. However, this would predict faster corrections to the rotational perturbations, which was not observed. Another potential influence in Experiment 1 is the rotational motion of the object, which could induce a corresponding rotation of the hand. Any transient response in the direction of object rotation would delay the adjustments toward the new grasp points, which was also not observed. Subjects appeared to respond to the appearance of a rotated object in the same way as to the appearance of a novel object. The abrupt changes in orientation may have been interpreted by the visuomotor system as changes in object shape, prompting re-computation of grasp points in the same way as when shape was perturbed. The appropriate contact points for grasping an object would generally depend on its position and orientation, so the process of grasp point selection might not take advantage of invariant representations of object shape.

While the perturbation responses observed here were sufficiently fast to allow smooth correction of grasp points, the response latencies were longer than in some other studies that tested orientation perturbations of a grasping target. Fan et al. (2006) observed a response latency of around 200 ms for 30° rotations of a pair of grip targets. Voudouris et al. (2013) tested 12° rotations of a cube during reach-to-grasp movements and observed rotations of the hand in the direction of object rotation after a delay of only 115 ms. We did not observe any rotation of the hand in the direction of perturbations in Experiment 1, but this difference could be due to the amount of object rotation. Voudouris et al. (2013) also observed some trials where subjects switched to new grasp points in response to perturbations. On these trials, adjustments toward the new grasp axis were detectable after 190 ms, which is still earlier than responses detected in our experiments.

The longer latencies observed here might have been due to the more complex visual processing required to determine new grasp axes for our stimuli. In Fan et al. (2006) and Voudouris et al. (2013), the same simple objects were repeatedly presented, so perturbation responses could be driven by the rotational motion of the target. In our conditions, the appropriate responses on perturbed trials were highly dependent on the particular shape of the target object, so visual analysis of shape would be required. Greenwald et al. (2005) measured responses to perturbations of slant information from texture during an object placement task, which also involves more complex processing of visual information. They observed response

latencies of around 250–300 ms, which is comparable to the latencies observed here. Visual shape analysis to determine grasp axes might require more processing time than reactions to translation or rotation of a target.

It is also possible that corrective responses began earlier than we were able to detect due to limited sensitivity of our analysis. One limiting factor is uncertainty in the predicted change in grasp axis on perturbed trials. The grasp points for individual objects on unperturbed trials had trial-to-trial variability, so the predicted change in grasp axis on a perturbed trial was an estimate based on average performance. Errors in these estimates and trial-to-trial variability around these means would add noise to the variables used for analysis of the perturbation effects. For the rotational perturbations used in Fan et al. (2006) and Voudouris et al. (2013), the expected responses were in a predictable direction, so this source of uncertainty was not present. Furthermore, the expected changes in grasp axes in our experiments were relatively small. The average angular difference between the predicted final grasp axes for initial stimuli and post-perturbation stimuli was 18.1° in Experiment 1 and 13° in Experiment 2. These are the expected differences in final grasp axes. Adjustment toward the final grasp axis occurs gradually over the course of movement even without perturbations, so the predicted differences at earlier points in the movement would be smaller. Small initial adjustments would be hard to detect given that there is noise in both the predictors and measurements.

We observed smooth corrective adjustments in grasp axis in response to shape perturbations, but this does not necessarily require continuous processing of shape information. The appearance of the new target object on perturbed trials might have prompted a reprogramming of the movement, using the same mechanisms involved in normal movement planning, followed by a gradual adjustment toward the new goals. Some previous studies have found that perturbations of target position or size during reaching to grasp an object can cause grip aperture to be double-peaked function over time (Paulignan et al. 1991b; Gentilucci et al. 1992), which have been interpreted as evidence for reprogramming of movement. However, Hesse and Franz (2009) have argued against this interpretation, noting that similar kinematics can also be observed without perturbations, and some other recent evidence suggests continuous control of grip aperture (Karak and Newport 2010). We did not observe any qualitative changes in the dynamics of movement on perturbed trials that would be indicative of a discrete change in the movement plan, but this could potentially be due to the small size of the required corrections and delay in the motor output. Our results demonstrate the ability to make online corrections in response to changes in object shape, but further research would be required to determine how these online corrections are implemented.

Neural correlates of shape processing for online control of grasping

Neurophysiological evidence suggests that the visuomotor system has mechanisms for visual shape processing that are distinct from the visual processing used for perceptual shape discrimination and object recognition (Goodale et al. 1991, 1994a, b; Milner and Goodale 1995). Such mechanisms could be responsible for the ability to make online adjustments to grasp points, as evidenced in our results.

The fact that the perturbation responses were automatic and relatively fast is consistent with the possibility of specialized shape processing for control of movements. We detected corrective responses to changes in object shape within 310–320 ms of the perturbation onset. Our analysis detected adjustments toward the expected grasp axes for the new target shape, which depended on the particular shapes, so the initial responses could not have been driven by simple motion signals. Electrophysiological studies have investigated neural processing during visual shape discrimination and observed ERP latencies of around 270–280 ms (Cui et al. 2000; Doniger et al. 2000; Schettino et al. 2011; Zhang et al. 2013). While this visual processing latency is less than the perturbation response latencies observed here, it would not leave much time for motor processing and translation to physical output. The delay between perturbation onset and detectable response includes not just the time required for visual processing of object shape, but also the time required to generate motor commands toward the new target grasp points, and the time before the motor commands produce measureable changes in the positions of the fingers. If selection of new grasp points were based on the visual shape processing revealed by EEG studies of shape discrimination, then the translation to physical changes would have to occur within 40 ms to produce the responses observed here, which is quite limited. This suggests that some other visual shape processing was involved.

Separate visual processing mechanisms for control of movement, as hypothesized by Goodale et al. (1994a, b), could account for this ability to make online adjustments in response to perturbations of a grasping target. Goodale and colleagues observed a double dissociation between a patient with severe visual agnosia and patients with optic ataxia (Goodale et al. 1991, 1994a, b; Milner and Goodale 1995). The agnostic was unable to perceptually discriminate objects with random 2D shapes, but picked up these objects at appropriate grasp points that varied with object shape in the same way as normal subjects. Patients with optic ataxia showed a reverse pattern of impairment: Shape discrimination judgments were accurate, but grasp points were not well adapted to the shape of the objects. This dissociation suggests that there is visual processing of shape information for online motor control that is distinct from

the visual processing that underlies shape perception. Such processing could be the basis for the perturbation responses observed here.

While the present results do not directly implicate the dorsal visual processing stream, variations of our method could potentially distinguish the contributions of dorsal and ventral processing in healthy people. One proposed distinction between these visual processing streams is that dorsal visual processing is unconscious and automatic. In a current follow-up study, we are testing whether similar perturbation responses can be elicited by unconscious visual feedback. Another possible variation is to vary the visual feedback in a manner that would selectively interfere with dorsal visual processing. For example, we are testing whether shapes defined by isoluminant or second-order contrast contours can support online corrections to grasping as observed here.

Real versus virtual grasping task

One limitation of our study is that we used a virtual grasping task: Subjects reached to touch the projected images of objects rather than picking up actual objects. Previous studies have observed different kinematics in pantomimed movements compared to actual reaching to grasp an object (e.g., Goodale et al. 1994b; Laimgruber et al. 2005; Westwood et al. 2000). Our virtual grasping task is more natural than a pantomimed movement in that subjects reach to touch a visible target on a physical surface. However, there are some potentially important differences compared to normal grasping. When picking up a real object, grasping at sub-optimal contact points would reduce the stability of the grip when the object was manipulated. For our virtual task, in contrast, there would be no cost to ‘grasping’ at sub-optimal contact points. Grasping real objects would also provide some implicit feedback about the effectiveness of different grasp points, while our virtual task allowed no such feedback. Thus, there is reason to expect that virtual grasping might be less sensitive to the constraints of object shape.

Despite the unnatural task demands, we found that the grasp points used for virtual grasping varied across objects in a manner consistent with optimal grasping. The grasp axes were consistently close to the center of mass of the objects, and force closure angles were lower than would be expected for random grasp axes. The grasp points observed in our study were also similar to grasp points used in previous studies using similar objects (Goodale et al. 1994a; Lederman and Wing 2003). The optimality of grasp axes observed in our experiments suggests that performance was guided by similar visuomotor mechanisms as when grasping real objects.

A previous study by Westwood et al. (2002) directly compared real grasping and virtual grasping of rectangular bars and found that there was a difference in the size

of the maximum grip aperture (MGA) relative to the final grip aperture (FGA). For a given FGA, the MGA was larger for grasping real bars than for virtual grasping. Westwood et al. suggest that subjects are able to adopt a less cautious approach to the virtual target, resulting in lower MGA/FGA ratio, because there is no danger of contacting the virtual bar incorrectly and no need to ensure perpendicular direction of force at contact. Consistent with these findings, the MGA/FGA ratio in our experiments was lower than would be expected for grasping of real objects. We observed an average MGA/FGA ratio of 1.2, while studies of actual grasping have observed MGA/FGA ratios of around 1.4–1.7 for objects with similar size (e.g., Eloka and Franz 2011; Westwood et al. 2002; Voudouris et al. 2013). Thus, there are at least some differences between the movement of the hand during virtual grasping and grasping real objects.

We performed a pilot study that tested both virtual grasping and grasping of real objects with the same shapes. As in Westwood et al. (2002), there was a difference in the MGA/FGA ratio, but the results were otherwise very similar for real and virtual grasping. The grasp axes for individual objects were similar in real and virtual conditions, and there was little difference in the optimality of grasp axes with respect to either torque control or force closure. While it remains possible that virtual grasping is not representative of normal grasping, the similarity of grasp axes suggests that similar shape processing underlies the selection of grasp points for virtual and real grasping.

Conclusion

Our results reveal that the visuomotor system is capable of online processing of shape information for identifying grasp points that would allow a stable grip. Perturbations of object orientation and shape during movement were used to isolate online processing. Subjects were able to smoothly adjust their movement in response to perturbations and achieve final grasp points that were appropriate for the shape of the target objects. The perturbations had minimal effect on either movement duration or the optimality of grasp points. These results demonstrate that effective hand adjustment could be made online during grasping. Corrective responses to perturbations were detectable within 310–320 ms, indicating relatively fast visual processing of object shape for control of grasping.

References

- Ansuini C, Santello M, Tubaldi F, Massaccesi S, Castiello U (2007) Control of hand shaping in response to object shape perturbation. *Exp Brain Res* 180(1):85–96
- Bingham GP, Muchisky MM (1993a) Center of mass perception and inertial frames of reference. *Percept Psychophys* 54(5):617–632
- Bingham GP, Muchisky MM (1993b) Center of mass perception: perturbation of symmetry. *Percept Psychophys* 54(5):633–639
- Blake A, Brady J (1992) Computational modelling of hand-eye coordination [and discussion]. *Philos Trans R Soc Lond B Biol Sci* 337(1281):351–360
- Bridgeman B, Lewis S, Heit G, Nagle M (1979) Relation between cognitive and motor-oriented systems of visual position perception. *J Exp Psychol Hum Percept Perform* 5(4):692
- Cui L, Wang Y, Wang H, Tian S, Kong J (2000) Human brain subsystems for discrimination of visual shapes. *NeuroReport* 11(11):2415–2418
- Desmurget M, Prablanc C (1997) Postural control of three-dimensional prehension movements. *J Neurophysiol* 77(1):452–464
- Doniger GM, Foxe JJ, Murray MM, Higgins BA, Snodgrass JG, Schroeder CE, Javitt DC (2000) Activation timecourse of ventral visual stream object-recognition areas: high density electrical mapping of perceptual closure processes. *J Cogn Neurosci* 12(4):615–621
- Eloka O, Franz VH (2011) Effects of object shape on the visual guidance of action. *Vision Res* 51(8):925–931
- Fan J, He J, Tillery SIH (2006) Control of hand orientation and arm movement during reach and grasp. *Exp Brain Res* 171(3):283–296
- Gentilucci M, Chieffi S, Scarpa M, Castiello U (1992) Temporal coupling between transport and grasp components during prehension movements: effects of visual perturbation. *Behav Brain Res* 47:71–82
- Glover S, Miall RC, Rushworth MF (2005) Parietal rTMS disrupts the initiation but not the execution of on-line adjustments to a perturbation of object size. *J Cogn Neurosci* 17(1):124–136
- Goodale MA, Milner AD, Jakobson LS, Carey DP (1991) A neurological dissociation between perceiving objects and grasping them. *Nature* 349:154–156
- Goodale MA, Meenan JP, Bühlhoff HH, Nicolle DA, Murphy KJ, Racicot CI (1994a) Separate neural pathways for the visual analysis of object shape in perception and prehension. *Curr Biol* 4(7):604–610
- Goodale MA, Jakobson LS, Keillor JM (1994b) Differences in the visual control of pantomimed and natural grasping movements. *Neuropsychologia* 32(10):1159–1178
- Greenwald HS, Knill DC (2009) A comparison of visuomotor cue integration strategies for object placement and prehension. *Vis Neurosci* 26:63–72
- Greenwald HS, Knill DC, Saunders JA (2005) Integrating visual cues for motor control: a matter of time. *Vision Res* 45(15):1975–1989. doi:10.1016/j.visres.2005.01.025
- Hesse C, Franz VH (2009) Corrective processes in grasping after perturbations of object size. *J Mot Behav* 41(3):253–273
- Kamp CVD, Bongers RM, Zaai FT (2009) Effects of changing object size during prehension. *J Mot Behav* 41(5):427–435
- Karok S, Newport R (2010) The continuous updating of grasp in response to dynamic changes in object size, hand size and distractor proximity. *Neuropsychologia* 48:3891–3900
- Kleinholdermann U, Franz VH, Gegenfurtner KR (2013) Human grasp point selection. *J Vis*. doi:10.1167/13.8.23
- Laimgruber K, Goldenberg G, Hermsdörfer J (2005) Manual and hemispheric asymmetries in the execution of actual and pantomimed prehension. *Neuropsychologia* 43(5):682–692
- Landsmeer JMF (1962) Power grip and precision handling. *Ann Rheum Dis* 21(2):164
- Lederman SJ, Wing AM (2003) Perceptual judgement, grasp point selection and object symmetry. *Exp Brain Res* 152(2):156–165
- Mamassian P (1997) Prehension of objects oriented in three-dimensional space. *Exp Brain Res* 114:235–245

- Milner AD, Goodale MA (1995) *The visual brain in action*. Oxford University Press, Oxford
- Napier JR (1956) The prehensile movements of the human hand. *J Bone Joint surg* 38(4):902–913
- Paulignan Y, MacKenzie CL, Marteniuk RG, Jeannerod M (1991a) Selective perturbation of visual input during prehension movements: the effects of changing object position. *Exp Brain Res* 83:502–512
- Paulignan Y, MacKenzie C, Marteniuk R, Jeannerod M (1991b) Selective perturbation of visual input during prehension movements: II. The effects of changing object size. *Exp Brain Res* 83(3):502–512
- Ponce J, Stam D, Faverjon B (1993) On computing two-finger force-closure grasps of curved 2D objects. *Int J Robot Res* 12(3):263–273
- Sanz PJ, Del Pobil AP, Inesta JM, Recatala G (1998) Vision-guided grasping of unknown objects for service robots. In: *Robotics and Automation, 1998. Proceedings of 1998 IEEE international conference on IEEE*, vol 4, pp 3018–3025
- Saunders JA, Knill DC (2003) Humans use continuous visual feedback from the hand to control fast reaching movements. *Exp Brain Res* 152(3):341–352. doi:[10.1007/s00221-003-1525-2](https://doi.org/10.1007/s00221-003-1525-2)
- Saunders JA, Knill DC (2004) Visual feedback control of hand movements. *J Neurosci* 24(13):3223–3234
- Saunders JA, Knill DC (2005) Humans use continuous visual feedback from the hand to control both the direction and distance of pointing movements. *Exp Brain Res* 162(4):458–473. doi:[10.1007/s00221-004-2064-1](https://doi.org/10.1007/s00221-004-2064-1)
- Schettino A, Loeys T, Delplanque S, Pourtois G (2011) Brain dynamics of upstream perceptual processes leading to visual object recognition: a high density ERP topographic mapping study. *Neuroimage* 55(3):1227–1241
- Seo NJ, Armstrong TJ (2009) Friction coefficients in a longitudinal direction between the finger pad and selected materials for different normal forces and curvatures. *Ergonomics* 52(5):609–616
- Tunik E, Frey SH, Grafton ST (2005) Virtual lesions of the anterior intraparietal area disrupt goal-dependent on-line adjustments of grasp. *Nat Neurosci* 8(4):505–511
- Voudouris D, Smeets JBJ, Brenner E (2013) Ultra-fast selection of grasping points. *J Neurophysiol* 110(7):1484–1489
- Westwood DA, Chapman CD, Roy EA (2000) Pantomimed actions may be controlled by the ventral visual stream. *Exp Brain Res* 130(4):545–548
- Westwood DA, Danckert J, Servos P, Goodale MA (2002) Grasping two-dimensional images and three-dimensional objects in visual-form agnosia. *Exp Brain Res* 144(2):262–267
- Zhang R, Hu Z, Zebi R, Zhang L, Li H, Liu Q (2013) Neural processes underlying the “same”-“different” judgment of two simultaneously presented objects—an EEG study. *PLoS One* 8(32):e81737